Prepublished Copy

NATURE ENVIRONMENT AND POLLUTION TECHNOLOGY

Article In Press

PEER-REVIEWED PREPUBLISHED MANUSCRIPT

This is a peer-reviewed prepublished version of the paper to be published in **Vol. 26, No. 1, March 2027.**

Assessing Urban Heat Island Intensity in a Desert Region: Case Study of Riyadh, Saudi Arabia

Julio Angeles Suazo, Marisol Paitan Iparraguirre, Roberto Angeles Vasquez, Carmencita Lavado Meza, Nataly Angeles Suazo, Leonel de la Cruz Cerrón, Leticia Leiva Arauco, Carmen Lavado Puente and Jairo Edson Gutiérrez Collao

RECEIVED
15 June 2026

CITE THIS ARTICLE
Suazo, J.A., Iparraguirre, M.P., Vasquez, R.A., Meza, C.L., Suazo, N.A., Cerrón, L.D.L.C., Arauco, L.L., Puente, C.L. and Collao, J.E.G., 2027. Assessing Urban Heat Island Intensity in a Desert Region: Case Study of Riyadh, Saudi Arabia. *Nature Environment and Pollution Technology*, 26(1), D1953.

https://doi.org/10.46488/NEPT.2027.v26i01.D1953

EARLY-ACCESS STATEMENT

This manuscript, after peer review, is being released online in its original, unedited form to provide early access to its findings. Prior to final publication, it will undergo additional editing and formatting. Readers may note that, as an unedited version, the manuscript may have linguistic and other minor errors. The DOI will be active after the final publication of the paper.

PUBLICATION STATUS

PEER REVIEW	ONLINE VERSION	FINAL ISSUE
Completed	**Prepublished**	**March 2027**

Original Research

Assessing Urban Heat Island Intensity in a Desert Region: Case Study of Riyadh, Saudi Arabia

Julio Angeles Suazo[1]; Marisol Paitan Iparraguirre[2]; Roberto Angeles Vasquez[3]; Carmencita Lavado Meza[1]; Nataly Angeles Suazo[4*]; Leonel de la Cruz Cerrón[5];Leticia Leiva Arauco[6]; Carmen Lavado Puente[6]; Jairo Edson Gutiérrez Collao[1]

[1] Universidad Nacional Autónoma de Tayacaja Daniel Hernández Morillo. Tayacaja, Perú jangelesambiental@gmail.com

[2]Universidad Alas Peruanas. Huancayo, Perú

[3] Universidad Nacional del Centro del Perú. Huancayo, Perú, roanvas@hotmail.com

[4] Universidad Tecnológica del Perú. Lima, Perú, nati2643@hotmail.com

[5] Universidad Continental. Huancayo, Perú, ldelacruz@continental.edu.pe

[6]Universidad Nacional Intercultural de la Selva Central Juan Santos Atahualpa, clavado@uniscjsa.edu.pe

Corresponding author: Nataly Angeles Suazo (Universidad Tecnológica del Perú); nati2643@hotmail.com

ORCID IDs of Authors

Julio Angeles Suazo; https://orcid.org/0000-0001-8327-9032

Roberto Angeles Vasquez; https://orcid.org/0000-0002-7248-912X

Carmencita Lavado Meza; https://orcid.org/0000-0003-1620-7180

Nataly Angeles Suazo; https://orcid.org/0000-0001-6144-0673

Leonel de la Cruz Cerrón; https://orcid.org/0000-0003-0935-3075

Carmen Lavado Puente: https://orcid.org/0000-0002-3061-0497

Jairo Edson Gutiérrez Collao: https://orcid.org/0000-0001-8984-6245

Abstract

This study proposes a quantile-based methodology for estimating Surface Urban Cold Island Intensity (SUCII) together with Surface Urban Heat Island Intensity (SUHII) over the Riyadh Metropolitan Area (RMA), Saudi Arabia, during the period 2001–2016. Two approaches were applied to quantify SUHII: the Gaussian fitting method proposed by Streutker (2002) and a quantile-based approach. In addition, a new quantile-based framework was developed to estimate SUCII using monthly Land Surface Temperature (LST) and annual Land Cover Type data derived from the MODIS sensor at a spatial resolution of 0.05°. The results reveal a clear seasonal alternation between daytime SUCI and nighttime SUHI conditions over the study area. The strongest daytime cooling occurred in September, whereas the highest daytime warming was observed in January, reflecting the seasonal influence of the surrounding desert environment on the urban–rural thermal contrast. Comparison with the Gaussian fitting approach showed that the proposed methodology consistently captured the seasonal evolution of surface thermal anomalies while avoiding ambiguities associated with the interpretation of negative intensity values. These findings demonstrate that the proposed framework provides a robust and reproducible approach for simultaneously characterizing urban heat and cold island phenomena in arid metropolitan regions and may support urban climate assessments and climate-sensitive urban planning.

Keywords

Cold island; Cuantil; Riad, Urban heat island

1. INTRODUCTION

Riyadh is one of the fastest-growing cities in the Middle East, experiencing rapid urban expansion and significant land-use changes over recent decades. A major environmental consequence of this urbanization process is the development of the Urban Heat Island (UHI) phenomenon, whereby urban areas exhibit higher air and surface temperatures than their surrounding rural or non-urban environments. UHI is widely recognized as one of the most pressing environmental challenges of the twenty-first century [1], [2]. Conversely, when urban areas are cooler than their surroundings, the phenomenon is referred to as the Urban Cold Island (UCI).

Elevated temperatures associated with UHIs can increase energy demand for cooling [3], exacerbate air pollution levels [4], [5], reduce outdoor thermal comfort, and negatively affect human health, potentially contributing to increased morbidity and mortality rates [6,7,8]. Recent studies have further highlighted the growing vulnerability of rapidly expanding cities in arid and semi-arid regions to heat-related risks and climate change impacts [9,10].

Urban Heat Island intensity is a thermal indicator that quantifies the localized increase in air or land surface temperatures resulting from anthropogenic modifications of the natural environment and the release of heat generated by human activities. Although UHI development is strongly linked to urban morphology and land-cover characteristics, its magnitude and spatial-temporal variability arise from complex, nonlinear interactions among multiple environmental and anthropogenic factors [11,12].

One of the primary drivers of UHI formation is thermal storage. Urban construction materials such as concrete, asphalt, and steel possess high thermal inertia, enabling them to absorb substantial amounts of solar energy during the day and release it as sensible heat during the night, thereby increasing nocturnal temperatures [13]. Another important factor is the reduction of evaporative cooling, as impervious urban surfaces generally retain less moisture than natural landscapes. Consequently, a larger fraction of the available energy is converted into sensible heat rather than latent heat, leading to higher surface and air temperatures [14].

Conversely, advective cooling mechanisms can mitigate urban warming. Temperature gradients between warmer urban areas and cooler rural surroundings may generate secondary circulations that transport cooler air into the city, thereby reducing urban temperatures [15]. Similarly, moderate to strong wind conditions can enhance heat dissipation and weaken UHI intensity. In addition, anthropogenic heat emissions from transportation, industrial activities, air-conditioning systems, and fossil fuel combustion contribute directly to urban warming [1].

Local climatic conditions also play a significant role in shaping urban thermal environments. For example, proximity to large water bodies can induce mesoscale circulations such as sea breezes, which may influence both UHI and UCI dynamics [16]. Recent research has shown that local climatic controls and urban greening strategies can substantially alter urban thermal patterns, particularly in hot-arid environments [17,18].

Negative values of the urban–rural temperature difference may indicate that urban surfaces are cooler than the surrounding rural areas, a condition generally referred to as the Urban Cold Island (UCI) effect. However, this interpretation depends on the methodology used to estimate urban thermal intensity. In studies based on the signed temperature difference, negative values correspond to UCI conditions, whereas positive values represent Urban Heat Island (UHI) conditions. In contrast, the methodology adopted in this study treats Surface Urban Heat Island Intensity (SUHII) and Surface Urban Cold Island Intensity (SUCII) as two independent positive quantities derived from the signed temperature difference. Consequently, negative intensity values are not used in the proposed framework; instead, the sign of ΔT identifies the thermal regime, while SUHII and SUCII quantify the magnitude of warming and cooling, respectively[19].

The daytime UCI effect is frequently associated with the presence of vegetation, which plays a critical ecological role in reducing urban temperatures through evapotranspiration and evaporative cooling. This cooling effect is particularly pronounced in desert cities, where irrigated parks and green spaces create a strong thermal contrast with the surrounding dry soils, sparse vegetation cover, and degraded suburban lands [20]. Recent studies have emphasized the effectiveness of urban greening interventions in mitigating extreme heat and enhancing thermal resilience in arid metropolitan regions [21,22].

In this context, the present study proposes a novel methodology for estimating Surface Urban Cold Island Intensity (SUCII) at a spatial resolution of 0.05° across the Riyadh Metropolitan Area (RMA) for the period 2001–2016. The proposed approach aims to improve the characterization of urban thermal dynamics in a rapidly expanding desert city and contribute to a better understanding of the spatiotemporal patterns of urban cooling processes.

2. MATERIALS AND METHODS

2.1. Site and location

The Riyadh Metropolitan Area (RMA) is located in the central region of the Kingdom of Saudi Arabia (Figure 1), approximately between 24.3°–25.1° N latitude and 46.3°– 47.2° E longitude. The metropolitan area covers approximately 1,973 km² and lies at an average elevation of about 600 m above sea level on the Najd Plateau.

Riyadh has a hot desert climate (BWh) according to the Köppen–Geiger climate classification, characterized by extremely hot, dry summers and mild winters. Mean maximum air temperatures frequently exceed 42 °C during summer (June–August), whereas winter minimum temperatures may decrease to approximately 11 °C. Annual precipitation is generally less than 100 mm and is concentrated during the winter and spring months, while cloud cover remains limited throughout most of the year, providing favorable conditions for satellite-based land surface temperature (LST) observations [23].

The Riyadh Metropolitan Area is the largest urban agglomeration and the administrative, economic, and political capital of Saudi Arabia. According to recent demographic statistics, the metropolitan population exceeds 7.5 million inhabitants, with an urbanization level greater than 99%, making Riyadh one of the fastest-growing cities in the Middle East. Rapid urban expansion during recent decades has replaced large areas of natural desert with impervious surfaces, substantially modifying the local surface energy balance and making the city an ideal case study for investigating the seasonal dynamics of Surface Urban Heat Island (SUHI) and Surface Urban Cold Island (SUCI) phenomena under arid climatic conditions [24].

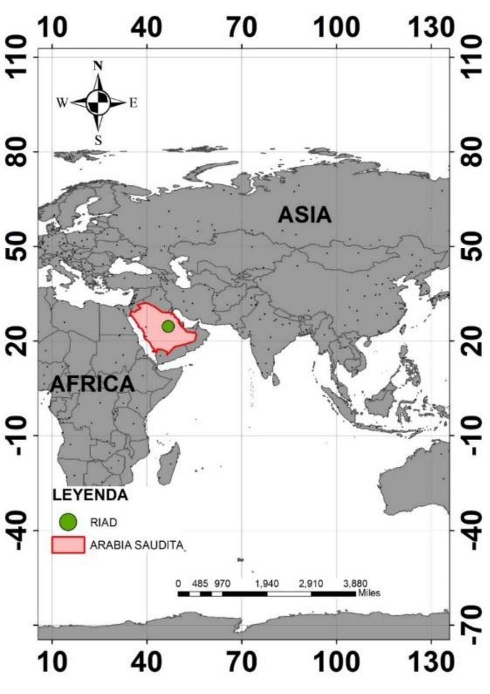

Fig. 1: Map ubication of MAR

2.2. MODIS data

Surface Land Surface Temperature (LST) data were obtained from the Moderate Resolution Imaging Spectroradiometer (MODIS) sensors [25] onboard the Terra and Aqua satellites. Monthly daytime and nighttime LST products, MOD11C3 (Terra) and MYD11C3 (Aqua), with a spatial resolution of 0.05° (approximately 5 km at the equator), were used to characterize the seasonal urban–rural thermal contrast over the Riyadh Metropolitan Area (RMA). Terra daytime and nighttime observations correspond to local overpass times of approximately 10:30 and 22:30, respectively, whereas Aqua observations correspond to approximately 13:30 and 01:30 local time. MODIS LST values were converted from the original digital units to degrees Celsius using the scale factor (0.02 K) provided in the product documentation.

To distinguish urban and rural surfaces, the MODIS Land Cover Type product (MCD12C1) at 0.05° spatial resolution was employed. Land-cover classes followed the International Geosphere–Biosphere Programme (IGBP) classification scheme, which includes 17 land-cover categories. Urban pixels were identified using the *Urban and Built-up* class, whereas rural pixels were selected from the surrounding desert areas after excluding urban cells. The same urban mask was applied throughout the study period to ensure temporal consistency.

Quality control followed the MODIS Quality Assurance (QA) layers. Only pixels flagged as good quality under clear-sky conditions were retained. Pixels with missing or poor-quality observations were excluded from the monthly analysis. Monthly LST fields were generated directly from the MOD11C3 and MYD11C3 products, and annual statistics were subsequently calculated from the monthly datasets. Terra and Aqua observations were initially analyzed independently to evaluate sensor consistency before any comparison or combined interpretation.

The study period extended from January 2001 to December 2016. Because the Aqua mission became operational in mid-2002, only Terra observations were available for the year 2001. Consequently, Terra data were used as the reference dataset for the complete study period, whereas Aqua observations were incorporated only for the years in which data were available. This procedure avoids introducing artificial gaps and ensures temporal consistency in the long-term analysis.

The surrounding rural environment is dominated by barren desert surfaces, as illustrated in Figure 2. This land-cover configuration strongly influences the seasonal thermal contrast between urban and rural areas. During daytime, the high thermal inertia and low evaporative capacity of desert surfaces frequently produce higher LST values than the urban core, resulting in Surface Urban Cold Island (SUCI) conditions. Conversely, during nighttime, the greater heat storage within urban materials promotes the development of Surface Urban Heat Island (SUHI) conditions.

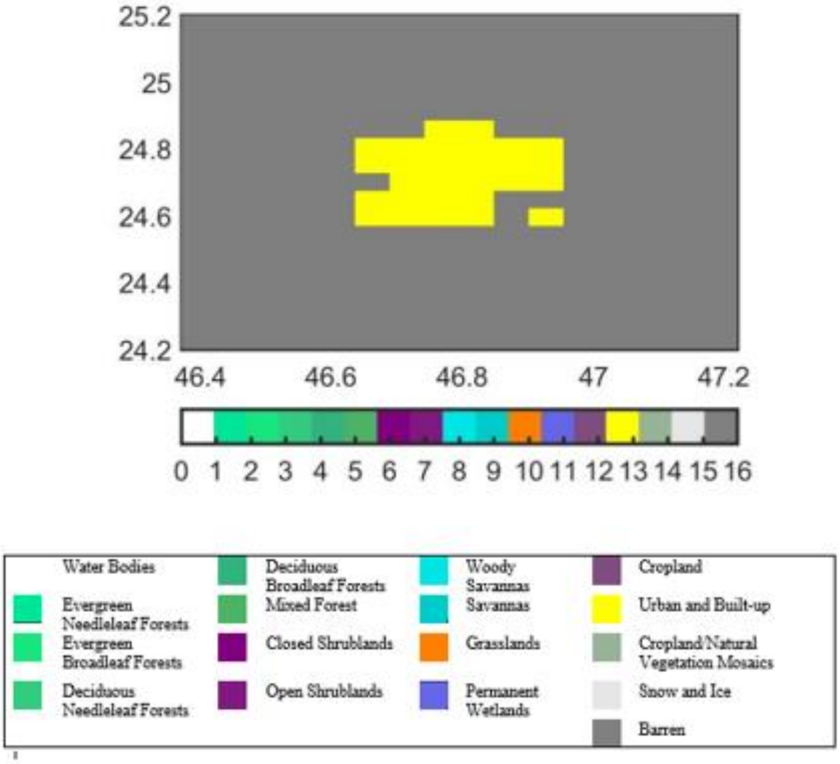

Fig. 2: Type of land cover according to the IGBP

2.3. SUHI estimation

To estimate SUHII, the method developed by[26], additionally, SUCII was determined using the quantile-based approach proposed by [27], which relies on the statistical comparison of surface temperature (ST) quantiles between urban and rural areas (e.g Suazo et al., 2025[28]).

2.4 Method proposed to estimation of SUCII

Proposal 1:

The following equation is only proposed when it presents months where the rural temperature (Tr) is higher than the urban temperature (Tu)

$$SUCII = Q_5^{rural} - Q_3^{urban}\ T_U < T_R \quad (1)$$

Following the quantile-based approach proposed by Flores (2016), Surface Urban Cold Island Intensity (SUCII) is estimated as the difference between the fifth rural temperature quantile Q_5^{rural} and the third urban temperature quantile Q_3^{urban} . This metric compares the warmest rural surfaces with the median thermal conditions of urban areas, allowing the identification of situations in which urban surfaces are cooler than their surrounding rural environment. Positive values indicate the presence of a Surface Urban Cold Island (SUCI), whereas negative values suggest the dominance of a Surface Urban Heat Island (SUHI).

Proposal 2:

Although for a metropolitan area that presents an island of cold and heat (F(T)) for different months it is proposed

$$F_i(T) = \{ \begin{matrix} Q_5^{urban} - Q_3^{rural} & T_U > T_R \\ Q_5^{rural} - Q_3^{urban} & T_U < T_R \end{matrix} \quad (2)$$

i: months

Also where Q_5^{urban} represents the upper urban temperature quantile, corresponding to the warmest urban surfaces, and Q_3^{rural} represents the median or reference rural temperature quantile. This approach emphasizes the thermal behavior of urban hotspots relative to the typical thermal conditions of the surrounding rural environment. Positive values indicate that urban areas are warmer than rural areas, characterizing a Surface Urban Heat Island (SUHI) effect

If the composite behavior of both phenomena (urban heat and cold island) is observed over a period of time

It will be used:

$$\sum_{i=1}^{12} F_i(T) = \sum_{j=1}^{12} (Q_5^{urbano} - Q_3^{rural} \ )_{T_U>T_R} + \sum_{k=1}^{12} Q_5^{rural} - Q_3^{urbano} \ )_{T_U<T_R} \ (3)$$

J: months where the condition is $T_U > T_R$

K: months where the condition is $T_U < T_R$

The annual thermal signal was obtained by summing the monthly SUHII and SUCII contributions separately. This approach enables a consistent characterization of the seasonal evolution of urban warming and cooling conditions while avoiding ambiguities associated with negative intensity values. Furthermore, the use of quantile-based temperatures instead of mean temperatures reduces the influence of outliers and provides a more robust representation of the urban–rural thermal contrast.

To characterize the annual urban–rural thermal contrast, a quantile-based thermal function $F_i(T)$ was computed by combining both Surface Urban Heat Island (SUHI) and Surface Urban Cold Island (SUCI) conditions. Following the quantile framework, when urban temperatures exceed rural temperatures $T_U > T_R$, the thermal anomaly is represented by the difference between the upper urban quantile and the reference rural quantile $Q_5^{urbano} - Q_3^{rural}$. Conversely, when urban temperatures are lower than rural temperatures (TU<TR), the anomaly is quantified as $Q_5^{rural} - Q_3^{urbano}$), representing Surface Urban Cold Island conditions.

Thus, the annual thermal signal is obtained by summing the monthly contributions of both warming and cooling regimes. This formulation allows the simultaneous characterization of the seasonal evolution of urban heat and urban cold island phenomena while reducing the influence of extreme values through the use of quantiles rather than mean temperatures.

3. RESULTS AND DISCUSSION

Figure 3 presents the classification of vegetation cover types within the Metropolitan Area of Riyadh (MAR) based on the IGBP methodology, for the years 2000 (A) and 2016 (B). As illustrated in the figure, different colors indicate various land cover types: yellow represents urban and built-up areas, grey indicates barren land and natural vegetation such as cropland, and purple corresponds to open and closed shrublands. In 2001, land cover in MAR was composed of approximately 70% barren land and 30% urban and built-up areas. By 2016, the proportion of urban and built-up land had increased to 34%, while barren land accounted for 66%.

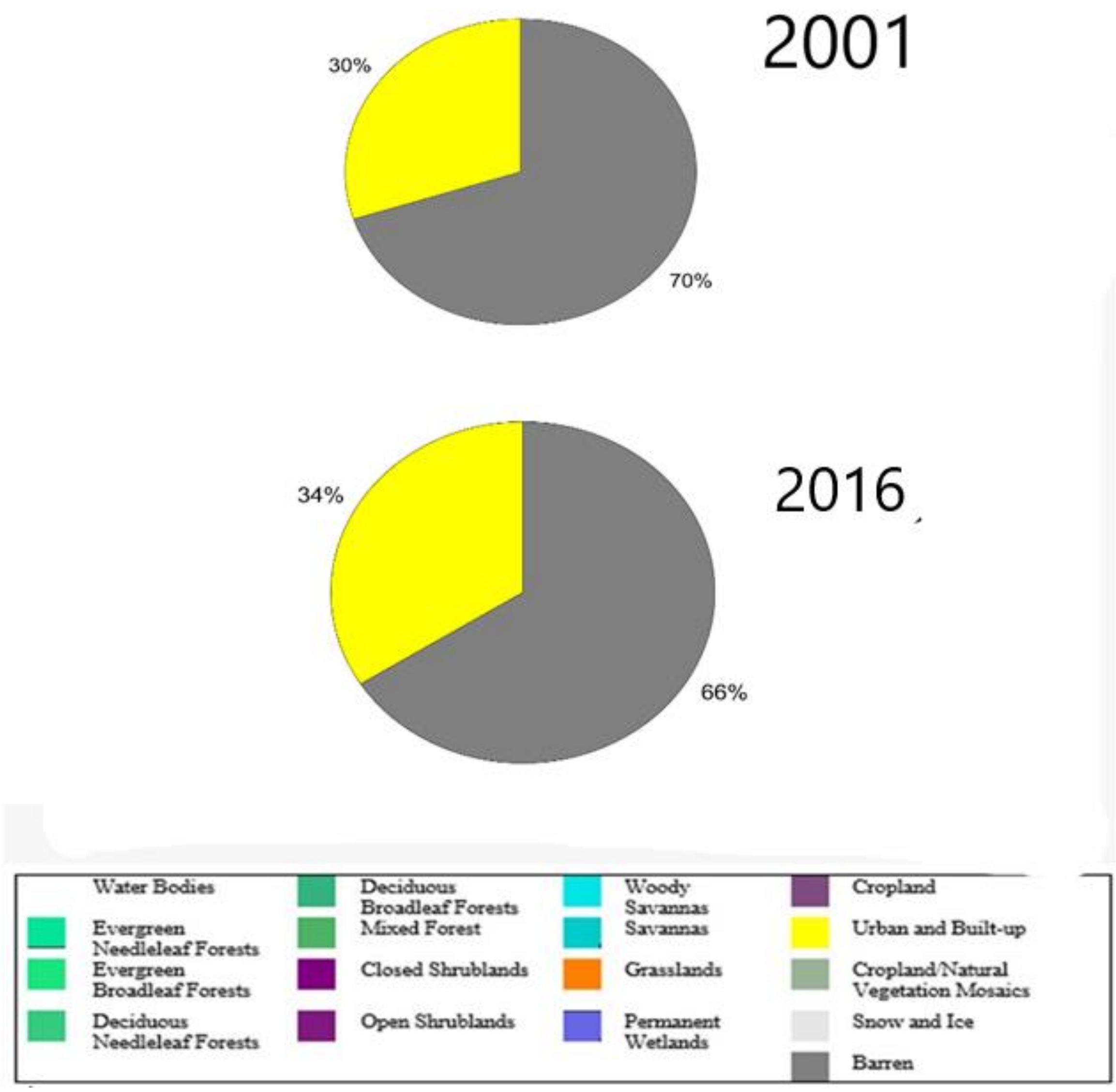

Fig. 3: Type of land cover for the MAT using the IGBP methodology for the 2001 (A) and 2016 (B) period.

3.2Vegetation Index and TS

To better understand the formation of SUHI intensities and the potential climate impacts of urban expansion, the relationship between Land Surface Temperature (TS) and vegetation indices specifically NDVI and EVI was examined. The analysis focused on the long-term monthly averages of these indices from 2001 to 2016 at two representative locations within the study area: one in the central urban zone and the other in a rural setting. As anticipated, vegetation index values were higher in urban areas and lower in rural ones. This pattern is due to the rural landscape being predominantly sandy, which retains heat efficiently. During daytime periods, a comparison between vegetation indices and TS reveals that urban areas with sparse vegetation tend to have higher surface temperatures. This phenomenon can partly be attributed to the fact that areas with smaller buildings and scattered vegetation allow for more unobstructed longwave radiation loss at night, leading to greater seasonal TS variability than in densely built-up urban centers (Hung et al., 2006). As shown in Figure 4, NDVI values remain nearly constant throughout the year, averaging around 0.08 in urban areas and about 0.01 in rural ones, with EVI following a similar trend.

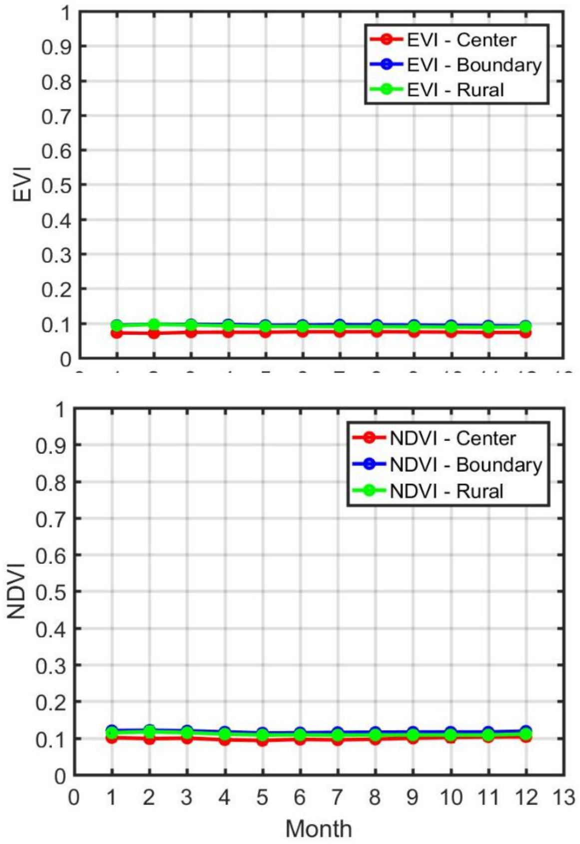

Fig 4: Evolucion annual de NDVI, EVI para la zona urbana y rural del AMR durante 2001-2016

Table 1 presents the long-term regression analyses (2001–2016) of NDVI vs. LST and EVI vs. LST for the Metropolitan Area of Riyadh (MAR), including slope values, intercepts, and correlation coefficients (R^2). In urban areas, the MAR exhibits strong positive correlations between LST and vegetation indices, with values ranging from 0.024 to 0.13. These positive slopes display seasonal variability, reaching their highest values in September and lowest in May. In contrast, rural areas show correlation values between 0.01 and 0.06. This pattern reflects the general cooling influence of vegetation on SUHI intensity.

Table 1. correlation indices (R2) of the regression lines between NDVI vs LST and EVI - LST for the MAR

Months	LST-NVI		LST-EVI	
	R2			
	URBAN	RURAL	URBAN	RURAL
January	0.064	0.005	0.11	0.009
February	0.078	0.001	0.10	0.003
March	0.024	0.006	0.056	0.001
April	0.046	0.001	0.049	0.001
May	0.023	0.003	0.068	0.001
June	0.054	0.001	0.08	0.011
July	0.062	0.001	0.10	0.019
August	0.065	0.001	0.11	0.018

September	0.13	0.001	0.16	0.021
October	0.071	0.001	0.081	0.003
November	0.032	0.001	0.061	0.007
December	0.036	0.001	0.053	0.004

3.3 Surface urban heat island using the Gaussian method

Table 2 presents the results for the long-term diurnal SUHII magnitudes (2001-2016) and the spatial extent for each month in the MAR, calculated using the Streutker method. The highest SUHII during the daytime was recorded in January (1.08°C), while the lowest occurred in September (-1.79°C). The largest spatial footprint was observed in April (8545.4 km²), and the smallest in June (140.6 km²), which corresponds to the formation of the SUHI.

Table 2. Diurnal mean of the SUHII and spatial extension with standard deviation for the MAR using the method developed by Streutker (2002) for the period 2001-2016. The table shows: magnitude of the SUHII: area of the formation footprint of the SUHI(km^2)

Month	FOOTPRINT AREA (km2)	SUHI
January	2554.6$\pm$9227	1.08$\pm$1.35
February	255.8$\pm$292	-1.35$\pm$2.03
March	1393.6$\pm$3100	-0.98$\pm$1.86
April	8545.4$\pm$33545	0.48$\pm$1.46
May	756.7$\pm$2031	-1.02$\pm$1.42
June	140.6$\pm$873	-1.21$\pm$1.05
july	479.9$\pm$982	-1.13$\pm$1.07
august	396.2$\pm$279	-1.28$\pm$0.52
September	208.3$\pm$532	-1.79$\pm$1.47
October	256.9$\pm$526	-1.70$\pm$0.49
November	618.2$\pm$1192	-0.84$\pm$1.54
december	1557$\pm$4694	0.50$\pm$1.43

To illustrate the seasonal variations of SUHII and SUCII in the MAR, Figure 3 displays the temporal evolution of Surface Temperature (ST) during both day and night for three different locations: urban, border, and rural. These graphs represent the long-term average values from 2001 to 2016. The daytime ST evolution (Figure 5A) reveals a distinct seasonal variation across the MAR, with similar temperature fluctuations at the central urban location and lower variations in rural areas. The highest daytime ST is recorded in August for the urban center (46°C), border (46°C), and rural areas (46°C). The lowest average temperatures are observed in January for all locations, with urban center (23°C), border (23°C), and rural (23°C) showing similar values. During the night (Figure 5B), the temporal evolution of LST shows seasonal changes with similar amplitudes across all locations, peaking in August at the central urban (33°C), border (30°C), and rural (28°C) areas. The lowest temperatures occur in January, with the urban center at 13°C, border at 12°C, and rural areas at 10°C.

Fig. 5: A. Time evolution of ST for daytime period and B. nighttime period of MAR in urban center, border and rural areas.

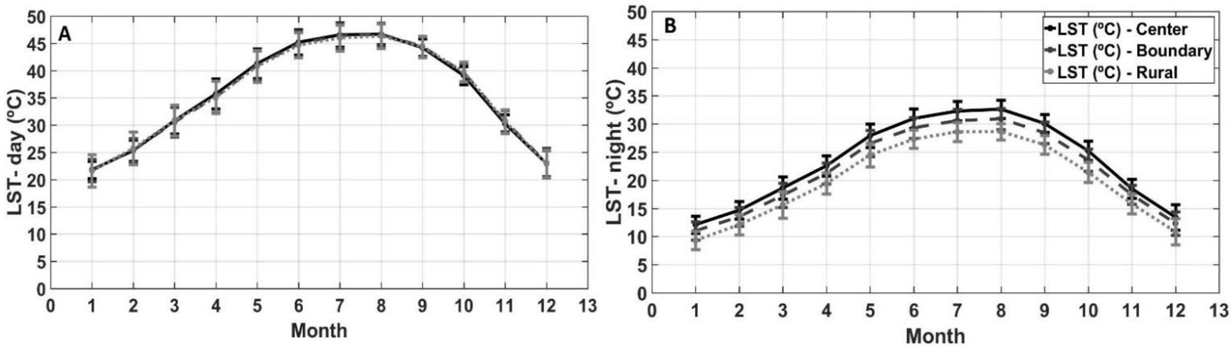

3.3 Daytime and nighttime SUHII and SUCII

From these it is observed that the diurnal SUHII (Figure 6A, B) is higher for the MAR in the summer months (December-February) and slightly lower in the months of May-August. Likewise, it is observed in figure 5D that the proposed method (eq. 3) is the one that best fits the streutker method due to the presence of both heat and cold islands phenomena for the period 2001-2016.

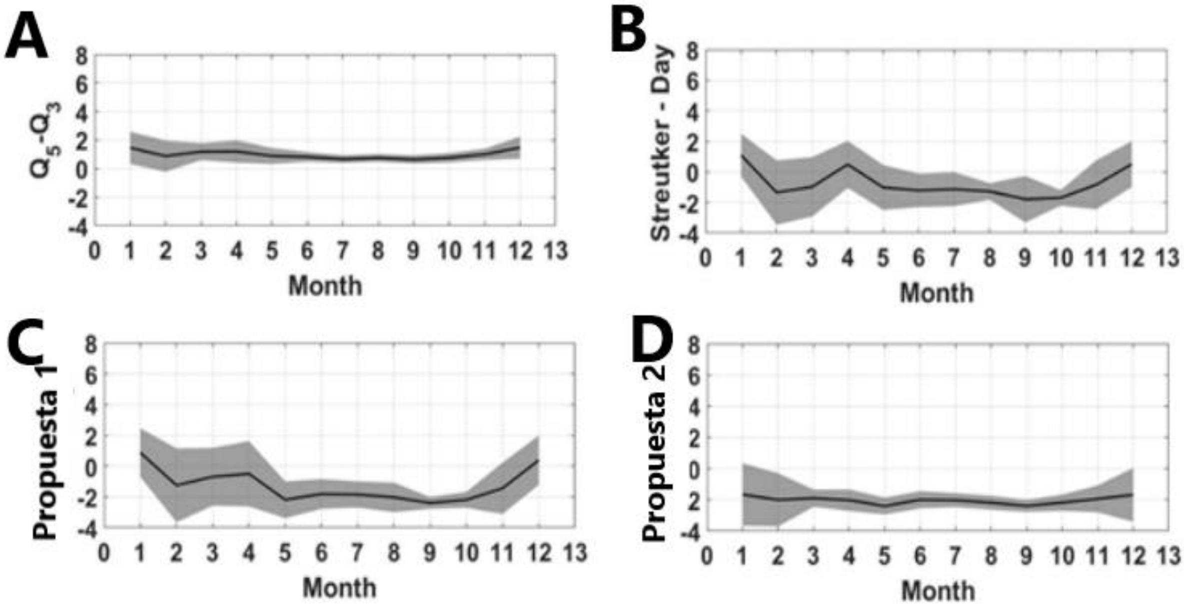

Fig. 6: A. Evolution Temporal from 2001-2016, monthly mean SUHII (° C) using the method of A. quantile, B. streutker and SUCII of methods C. proposed 1 and D. proposed 2 for the MAR.

For the MAR, the results obtained using the statistical method outlined in equation 3 for diurnal periods are presented in Table 3. The diurnal SUHII reaches its highest value in January (0.87°C) and its lowest value in September (-2.38°C). When comparing the SUHII results from both methods (Tables 2 and 3), a strong level of consistency is observed between the two.

Table 3. Daytime monthly average of ST (° C) with its standard deviation for rural and urban areas and the SUHII (° C) at 5 km resolution for the MAR during the period 2001 - 2016.

Period diurnal				Period nocturnal	
Month	Method cuantil	Method proposed (eq.1)	Method proposed (eq. 3)	Method cuantil	Method Streutker
January	1.45±1.13	-1.66±2.0	0.87±1.57	4.12±0.51	4.57±0.51
February	0.87±1.09	-2.00±1.7	-1.24±2.39	4.24±0.57	4.59±0.61
March	1.18±0.59	-1.89±0.55	-0.68±1.87	4.45±0.52	4.88±0.57
April	1.20±0.78	-2.02±0.68	-0.49±2.12	4.31±0.66	4.77±0.65
May	0.89±0.56	-2.40±0.54	-2.18±1.19	4.54±0.49	5.08±0.51
June	0.82±0.34	-2.00±0.55	-1.80±0.96	4.72±0.45	5.30±0.45
july	0.67±0.27	-2.02±0.45	-1.83±0.85	4.74±0.27	5.28±0.29

august	0.75±0.27	-2.19±0.44	-2.02±0.95	4.96±0.44	5.50±0.44
September	0.64±0.29	-2.38±0.38	-2.38±0.39	5.20±0.28	5.81±0.30
October	0.76±0.33	-2.18±0.52	-2.18±0.52	5.32±0.41	5.87±0.38
November	1.00±0.39	-1.94±0.86	-1.43±1.67	4.28±0.66	4.66±0.68
december	1.47±0.77	-1.68±1.7	0.38±1.59	4.00±0.67	4.35±0.75

Likewise, the results using the statistical method of quantiles in the night periods are shown in Table 3. The nocturnal SUHII obtained with the quantile method, present maximum values in October (5.32 ° C) and minimum values in December (4.0 °C).

3. DISCUSSION

the results reveal a pronounced seasonal variability in the urban–rural thermal contrast over the riyadh metropolitan area (rma), characterized by the predominance of surface urban cold island (suci) conditions during daytime in the warm season and surface urban heat island conditions during nighttime. this seasonal reversal is a common feature of arid and hyper-arid cities, where the magnitude and even the sign of the thermal anomaly depend strongly on the definition of urban and rural reference areas, the surrounding land-cover composition, and the spatial heterogeneity of the landscape [29]. recent global analyses demonstrated that nearly half of the world's arid cities exhibit a daytime transition from suhi to suci depending on the methodology used to define urban and rural domains, highlighting the importance of methodological consistency when estimating thermal contrasts.

the daytime warming observed in january and the cooling detected in september can be interpreted in terms of seasonal variations in the surface energy balance. during late summer, the surrounding barren desert experiences intense solar heating because of its low soil moisture, limited evapotranspiration, sparse vegetation cover, and high sensible heat fluxes. consequently, rural desert surfaces frequently become warmer than the urban core, producing daytime suci conditions. in contrast, winter months receive lower incoming solar radiation and exhibit reduced thermal gradients between urban and rural surfaces, thereby weakening the daytime cooling effect. similar seasonal behavior has been reported in riyadh and other desert cities, where daytime thermal contrasts are strongly controlled by soil moisture availability, vegetation abundance, albedo, and surface material properties [29].

The magnitudes estimated in the present study are comparable to those reported for other hot-arid metropolitan areas. for riyadh, recent studies reported daytime suci intensities between approximately −0.3 and −1.6 °c and nighttime suhi intensities ranging from 2.8 to 3.4 °c, depending on the selection of the rural reference area. similar daytime cooling and nighttime warming have also been documented for desert cities such as dubai, abu dhabi, phoenix, and several arid cities in northern china, demonstrating that the coexistence of suci and suhi is a characteristic feature of desert urban environments rather than an isolated phenomenon [29,30,31].

Several environmental factors may contribute to the observed thermal behavior. vegetation and irrigated landscapes increase latent heat flux through evapotranspiration, reducing daytime land surface temperatures, whereas highly reflective materials increase surface albedo and decrease absorbed solar radiation. conversely, barren soils, sparse vegetation, low soil moisture, atmospheric dust loading, and extensive impervious surfaces increase sensible heat fluxes and enhance daytime warming. urban morphology, including building density, street orientation, and canyon geometry, also influences radiative trapping and nocturnal heat storage, thereby intensifying nighttime suhi [29,32]

Comparison between the gaussian fitting method and the proposed quantile-based approach indicates that both techniques reproduce similar seasonal thermal patterns despite their different conceptual assumptions. the gaussian approach estimates an idealized continuous thermal surface through parametric fitting, whereas the quantile-based framework derives thermal intensity directly from the statistical distribution of observed land surface temperatures. consequently, discrepancies between both methods are expected during transition months characterized by greater spatial heterogeneity and mixed thermal conditions rather than indicating methodological inconsistency. similar methodological sensitivities have recently been discussed for arid cities, where estimated suhi intensity varies according to the urban mask, rural definition, and statistical methodology adopted. Several limitations should be acknowledged. first, the modis lst products have an effective spatial resolution of approximately 5 km, implying that individual pixels frequently contain mixtures of urban surfaces, bare soil, and transitional land-cover classes. this mixed-pixel effect may underestimate the true urban–rural thermal contrast. second, thermal infrared observations are restricted to clear-sky conditions; therefore, the reported suhi and suci intensities represent only cloud-free situations and may not capture the complete range of atmospheric variability. third, the estimated thermal contrast depends on the definition of the rural reference area, which has recently been identified as one of the principal sources of uncertainty in suhi studies conducted in arid regions. finally, although the proposed quantile-based framework reduces the influence of extreme observations, the resulting estimates remain sensitive to the selected quantile thresholds and the adopted urban mask. Overall, the proposed quantile-based methodology provides a robust framework for simultaneously characterizing surface urban heat island (suhi) and surface urban cold island conditions while avoiding ambiguities associated with signed thermal differences.

nevertheless, the conclusions should be interpreted within the limitations imposed by the spatial resolution of modis observations and the absence of independent in situ validation. future studies should integrate higher-resolution thermal imagery, field observations, and environmental variables such as albedo, vegetation indices, soil moisture, irrigation intensity, and urban morphology to improve the physical interpretation of seasonal thermal dynamics in arid metropolitan environments.

4. CONCLUSIONS

The results indicate that the Riyadh metropolitan area exhibits pronounced seasonal variability in its surface urban thermal behavior. during the daytime, the proposed surface urban heat island intensity and surface urban cold island intensity indicators identified the highest urban warming conditions in january and the strongest urban cooling conditions in september. these findings suggest that the urban thermal environment of Riyadh is characterized not only by surface warming but also by recurrent urban cooling episodes, reflecting the complex urban–rural thermal interactions that occur in arid environments.

The comparison between the gaussian fitting approach and the proposed quantile-based methodology indicates that the principal differences arise from the thermal behavior of the surrounding rural desert. in particular, rural land surface temperatures do not always satisfy the assumptions of homogeneous or linearly varying background temperatures adopted by conventional SUHI methods. during several periods of the year, barren desert surfaces become warmer than the urban area because of their low soil moisture, limited vegetation, and high solar heating, making the interpretation of conventional signed UHI estimates less straightforward.

The proposed methodology addresses this limitation by explicitly distinguishing between surface urban heat island and surface urban cold island regimes. by deriving both indicators from a signed urban–rural temperature difference while reporting their intensities as independent positive quantities, the method provides a consistent representation of seasonal urban thermal dynamics and avoids ambiguities associated with negative UHI values. this feature is particularly relevant for arid and semi-arid metropolitan regions, where daytime urban cooling and nighttime urban warming frequently coexist.

Despite these advantages, several limitations should be acknowledged. the analysis is based on modis land surface temperature products with a spatial resolution of approximately 5 km, which may introduce mixed-pixel effects in heterogeneous urban environments. furthermore, the thermal observations are restricted to clear-sky conditions, and the estimated thermal contrasts depend on the definition of the urban and rural masks as well as the selected quantile thresholds. in addition, the proposed methodology has not yet been independently validated using ground-based observations or higher-spatial-resolution thermal imagery.

Future research should evaluate the performance of the proposed framework using independent meteorological observations and high-resolution satellite data, such as landsat or ecostress, and examine its applicability across different climatic regions and urban morphologies. incorporating additional environmental variables, including vegetation indices, albedo, soil moisture, irrigation intensity, and urban morphology, would also improve the physical interpretation of the mechanisms controlling surface urban heat island and surface urban cold island dynamics. these developments would further strengthen the applicability of the proposed methodology for urban climate assessment, heat mitigation planning, and sustainable urban development in arid cities.

5. PATENTS

Acknowledgments: The surface temperature data sets were obtained from NASA from their website at: http://modis.gsfc.nasa.gov/

Conflicts of Interest: The authors declare no conflicts of interest.

REFERENCES

[1] H. Taha, "Urban climates and heat islands: Albedo, evapotranspiration, and anthropogenic heat," *Energy Build.*, vol. 25, no. 2, 1997, doi: 10.1016/s0378-7788(96)00999-1.

[2] T. R. Oke, "City size and the urban heat island," *Atmos. Environ.*, vol. 7, no. 8, 1973, doi: 10.1016/0004-6981(73)90140-6.

[3] M. Kolokotroni, X. Ren, M. Davies, and A. Mavrogianni, "London's urban heat island: Impact on current and future energy consumption in office buildings," *Energy Build.*, vol. 47, 2012, doi: 10.1016/j.enbuild.2011.12.019.

[4] C. Sarrat, A. Lemonsu, V. Masson, and D. Guedalia, "Impact of urban heat island on regional atmospheric pollution," *Atmos. Environ.*, vol. 40, no. 10, 2006, doi: 10.1016/j.atmosenv.2005.11.037.

[5] Q. Weng and S. Yang, "Urban air pollution patterns, land use, and thermal landscape: An examination of the linkage using GIS," *Environ. Monit. Assess.*, vol. 117, no. 1–3, 2006, doi: 10.1007/s10661-006-0888-9.

[6] R. Basu and J. M. Samet, "Relation between elevated ambient temperature and mortality: A review of the epidemiologic evidence," *Epidemiologic Reviews*, vol. 24, no. 2. 2002, doi: 10.1093/epirev/mxf007.

[7] S. Mărgulescu *et al.*, "Characteristics of buoyant flow from open windows in naturally ventilated rooms," *Energy Build.*, vol. 40, no. 2, 2014.

[8] J. Klenk, C. Becker, and K. Rapp, "Heat-related mortality in residents of nursing homes," *Age Ageing*, vol. 39, no. 2, 2010, doi: 10.1093/ageing/afp248.

[9] Zhang, P., Wang, Y., Li, D., & Zhao, C. (2023). Urban heat island intensification and climate resilience in rapidly growing desert cities. *Science of the Total Environment, 891*, 164410. https://doi.org/10.1016/j.scitotenv.2023.164410.

[10] Li, X., Zhou, Y., Asrar, G. R., Imhoff, M., & Li, X. (2022). The surface urban heat island response to urban expansion: A global assessment. *Environmental Research Letters, 17*(3), 034028. https://doi.org/10.1088/1748-9326/ac4f6d

[11] T. R. Oke, "The energetic basis of the urban heat island," *Q. J. R. Meteorol. Soc.*, 1982, doi: 10.1002/qj.49710845502.

[12] A. J. Arnfield, "Two decades of urban climate research: A review of turbulence, exchanges of energy and water, and the urban heat island," *Int. J. Climatol.*, vol. 23, no. 1, 2003, doi: 10.1002/joc.859.

[13] P. Ramamurthy *et al.*, "Influence of subfacet heterogeneity and material properties on the urban surface energy budget," *J. Appl. Meteorol. Climatol.*, vol. 53, no. 9, 2014, doi: 10.1175/JAMC-D-13-0286.1.

[14] D. J. Sailor, "A green roof model for building energy simulation programs," *Energy Build.*, vol. 40, no. 8, 2008, doi: 10.1016/j.enbuild.2008.02.001.

[15] M. Haeger-Eugensson and B. Holmer, "Advection caused by the urban heat island circulation as a regulating factor on the nocturnal urban heat island," *Int. J. Climatol.*, vol. 19, no. 9, 1999, doi: 10.1002/(SICI)1097-0088(199907)19:9<975::AID-JOC399>3.0.CO;2-J.

[16] P. Vahmani and G. A. Ban-Weiss, "Impact of remotely sensed albedo and vegetation fraction on simulation of urban climate in WRF-urban canopy model: A case study of the urban heat island in Los Angeles," *J. Geophys. Res.*, vol. 121, no. 4, 2016, doi: 10.1002/2015JD023718.

[17] Yang, J., Ren, J., Sun, D., Xiao, X., Xia, J., Jin, C., & Li, X. (2024). Urban greening and heat mitigation in hot-arid cities under climate change. *Sustainable Cities and Society, 102*, 105184. https://doi.org/10.1016/j.scs.2024.105184

[18] Luo, X., Peng, Y., Guan, K., Wang, S., & Zhang, Y. (2021). Impacts of urbanization and vegetation changes on urban thermal environments in arid regions. *Remote Sensing, 13*(18), 3654. https://doi.org/10.3390/rs13183654

[19] J. Yang, K. W. Tham, S. E. Lee, M. Santamouris, C. Sekhar, and D. K. W. Cheong, "Anthropogenic heat reduction through retrofitting strategies of campus buildings," *Energy Build.*, vol. 152, 2017, doi: 10.1016/j.enbuild.2016.11.051.

[20] M. Georgescu, M. Moustaoui, A. Mahalov, and J. Dudhia, "An alternative explanation of the semiarid urban area 'oasis effect,'" *J. Geophys. Res. Atmos.*, vol. 116, no. 24, 2011, doi: 10.1029/2011JD016720.

[21] Jiang, Y., Zhao, L., Li, X., & Zhou, W. (2022). Cooling effects of urban green infrastructure on land surface temperature in arid environments: A global review. *Urban Forestry & Urban Greening, 74*, 127650. https://doi.org/10.1016/j.ufug.2022.127650

[22] He, B. J., Zhao, D. X., Xiong, K., Qi, J. D., Ulpiani, G., Pignatta, G., & Jones, P. (2023). Urban heat island mitigation: A review of strategies and future perspectives in arid and semi-arid cities. *Sustainable Cities and Society, 95*, 104617. https://doi.org/10.1016/j.scs.2023.104617

[23] General Authority for Statistics (Saudi Arabia) (2024). *Population statistics of Riyadh Metropolitan Area.*

[24] World Bank. (2024). *Urban population (% of total population) – Saudi Arabia*

[25] A. Schneider, M. A. Friedl, D. K. McIver, and C. E. Woodcock, "Mapping Urban Areas by Fusing Multiple Sources of Coarse Resolution Remotely Sensed Data," *Photogrammetric Engineering and Remote Sensing*,

vol. 69, no. 12. 2003, doi: 10.14358/PERS.69.12.1377.

[26] D. R. Streutker, “A remote sensing study of the urban heat island of Houston, Texas,” *Int. J. Remote Sens.*, 2002, doi: 10.1080/01431160110115023.

[27] J. L. Flores R., A. J. Pereira Filho, and H. A. Karam, “Estimation of long term low resolution surface urban heat island intensities for tropical cities using MODIS remote sensing data,” *Urban Clim.*, 2016, doi: 10.1016/j.uclim.2016.04.002.

[28] Suazo, J.A., Vasquez, R.A., Meza, C.L., Suazo, N.A., de la Cruz Cerrón, L., Mitma, P.M., Rojas, J.F. and Abi Karam, H., 2025. Superficial Urban Heat Island in the City of Santos, Brazil. *Nature Environment and Pollution Technology*, *24*(4), pp.1-7. https://doi.org/10.46488/NEPT.2025.v24i04.D1776

[29] Alghamdi, A. S. (2025). An integrated ML-powered geospatial analysis of surface urban heat island and its mitigation in Riyadh City, Saudi Arabia. Urban Climate, 64, 102642. https://doi.org/10.1016/j.uclim.2025.102642

[30] Zhou, D., Xiao, J., Bonafoni, S., Berger, C., Deilami, K., Zhou, Y., Frolking, S., Yao, R., Qiao, Z., & Sobrino, J. A. (2019). Satellite remote sensing of surface urban heat islands: Progress, challenges, and perspectives. Remote Sensing, 11(1), 48. https://doi.org/10.3390/rs11010048

[31] Wang, J., Lu, L., Zhou, X., Huang, G., & Chen, Z. (2025). Spatio-Temporal Patterns and Drivers of the Urban Heat Island Effect in Arid and Semi-Arid Regions of Northern China. Remote Sensing, 17(8), 1339. https://doi.org/10.3390/rs17081339

[32] Yuan, Y., Santamouris, M., Xu, D., Geng, X., Li, C., Cheng, W., Su, L., Xiong, P., Fan, Z., Wang, X., & Liao, C. (2025). Surface urban heat island effects intensify more rapidly in lower income countries. npj Urban Sustainability, 5, 11.